Materials Today Communications xxx (xxxx) xxx

Contents lists available at ScienceDirect

Materials Today Communications

journal homepage: www.elsevier.com/locate/mtcomm

Ultrafast femtosecond laser micro-marking of single-crystal natural diamond by two-lens focusing system

Yasir F. Joya [a,b,*], Bing Yan [a], Kelvin James [c], Liyang Yue [a], Simon C. Middleburgh [d], Zengbo Wang [a,*]

[a] School of Computer Science and Electronic Engineering, Bangor University, Bangor, LL57 1UT, United Kingdom
[b] Faculty of Materials and Chemical Engineering, Ghulam Ishaq Khan Institute of Engineering Sciences and Technology, Topi (23640), Khyber Pakhtunkhwa, Pakistan
[c] The Diamond Center Wales Ltd, Talbot Green, Rhondda Cynon Taff, CF72 9FG, United Kingdom
[d] Nuclear Futures Institute, Bangor University, LL57 1UT, United Kingdom

ARTICLE INFO

Keywords:
Ultrafast laser
Natural diamond
Laser ablation
Raman spectroscopy
Security marking

ABSTRACT

The inscription of unique logo and security marking on diamonds and gemstones is in high demand by worldwide manufacturers and businesses for anti-counterfeiting purposes and traceability. Short pulsed lasers enable marking of transparent materials, challenge remains to produce digital security micro-features on thin facets of the natural diamond in a non-intrusive manner. We propose the design and demonstration of a novel two-lens focusing system to inscribe diamond at microscale and high throughput by an ultrafast laser scanning process. A threshold laser fluence of ~2.5 J/cm^2 and a scan speed of 2 mm/s realized writing of high-contrast data matrix code and serial number without inducing defects and cracking in the diamond. Characterization revealed smooth ablation depth profile with distinct laser-induced periodic surface structures (LIPSS) in the laser inscribed regions determined through scanning electron microscopy (SEM) and 3D optical microscopy. Raman spectroscopy revealed diamond cubic structure dominating with mixing of graphitic structure in the laser markings at various scanning speeds. Comparing with the 0.05 NA f-theta lens, the two-lens focusing system offered 7x improvement in the marking resolution (3 μm in line-width) in addition to its simplicity and add-on flexibility to industrial laser marking systems.

1. Introduction

Owing to its highest stiffness, excellent thermal properties and large refractive index, diamond is an attractive material for tool manufacturing, semiconductor applications, electrical components, in addition to the jewelry industry. Natural diamonds are cut and produced in variety of shapes, sizes and geometries to suit a widespread consumer base. Their gradually rising demand and greater value, compared to other gems, have culminated into inventing measures for decentralized record keeping, transparency and track and trace procedures to avoid counterfeiting and improve sustainability by relying on modern QR-code and Internet of Things (IoT) technologies [1,2]. In the quest of such a smart system, new and improved industrial processes to print machine-readable digital features on diamonds and precious stones are of immense interest.

Although, several conventional technologies are available for surface marking and inscribing of industrial products, marking by lasers is unique in the sense it is quick, more reliable and automated. Therefore, many industries and businesses have been adopting these for scribing serial marking on gemstones in a user-friendly and viable process without influencing their surface quality. Nanosecond (ns) pulsed lasers, such as excimer lasers (wavelength 193−355 nm), have demonstrated success to ablate and mark a variety of optically transparent materials due to their greater absorption coefficient [3]. However, material processing by these ns-lasers is accompanied by low ablation rate and induced photo-thermal effects [4,5] challenging high-resolution and defect-free microscale processing of diamonds.

Due to their shorter pulse duration and high peak power compared to ns-lasers, ultrafast lasers enable cold processing (interaction times shorter than the electron/phonon coupling time) leading to the enhanced micromachining quality of a wide range of industrial materials [6,7]. A widespread research interest has been devoted to the synthetically grown single-crystal diamond (SCD) and its microstructural modification by ultrafast laser processing [8–10]. Meanwhile,

* Corresponding authors.
E-mail addresses: yasir.joya@outlook.com (Y.F. Joya), z.wang@bangor.ac.uk (Z. Wang).

https://doi.org/10.1016/j.mtcomm.2020.101800
Received 14 September 2020; Accepted 19 October 2020
Available online 2 November 2020

work in the field of fs-laser based micro-processing of natural diamonds and gems has been overgrowing due to global concern for safe keeping as well as fast-track traceability through digital marking. Ionin et al. first reported on fs-laser writing of linear patterns at different powers and focal depths inside the natural bulk diamond at the pulse repetition rate of 10 Hz [11]. Recently, Gomes et al. demonstrated the ultrafast laser inscription of QR-codes on diamond, ruby and sapphire [12]. A low repetition rate fs-laser (1 kHz) was used to inscribe QR-code consisting of microdots on the natural diamond to overcome defect clusters and graphitization. Table 1 lists the results obtained from previous reports and compares the laser processing parameters adopted for various types of diamonds.

We report a new fs-laser scanning process by writing alphanumeric labels and identifiable security code on the polished facet of the natural diamond (derived from standard gem cutting and polishing) in ambient condition. A novel design for focused laser scanning has been applied and marking of serial number and data matrix code, 25−100 μm in height, is successfully demonstrated. The add-on 0.60 NA focusing objective led to 7-fold improvement in the marking resolution (i.e. 3 μm) compared to the focusing by conventional 0.05 NA f-theta lens (i.e. 20 μm). Meanwhile, the proposed focusing setup is user-friendly and flexible to add-on to the commercial laser marking systems saving significant time and cost to the product marking.

2. Material and methods

Natural diamond samples with polished facets in specific size and cut profile were received from Diamond Centre Wales Ltd. (DCW) for laser processing. Fig. 1 shows the typical schematic drawing of the diamond indicating its various edges, facets and dimensions. The samples were associated to type-1a i.e. containing nitrogen as a trace element/natural impurity within the pure carbon lattice. The size and grade of each diamond were measured as: marquise and emerald cut; depth and width of 2−3 mm, length of 3−4 mm. Approximate total weight of the received samples was measured as 0.3 cts (i.e. ~60 mg) only.

The samples were ultrasonically cleaned in ethanol for 5 min followed by cleaning in deionized water for 5 min and then dried in the ambient air. Those were held onto a clean glass slide by re-usable putty and orientated so that the facet was able to be laser irradiated and kept at 90 degrees to the laser beam propagation. The laser processed samples were subsequently cleaned using the same process described for pre-irradiation and characterization of the marked area was carried out as follows.

2.1. Laser marking setup

The ultrashort pulses were generated through a fs-laser micro-machining system consisting of a Ti:Sapphire oscillator (Spectra Physics Mai Tai) and a regenerative amplifier (Spectra Physics Hurricane) delivering 100 fs-pulses at 800 nm wavelength and 5 kHz repetition rate with the pulse energy up to 200 μJ (1 W). The collimated laser beam (Gaussian profile) was focused through an f-theta lens (NA 0.05) to 20 μm spot size on the sample (Fig. 2(a)). Linearly polarized fs-laser beam was used, and pulse energy was varied using attenuator fixed in

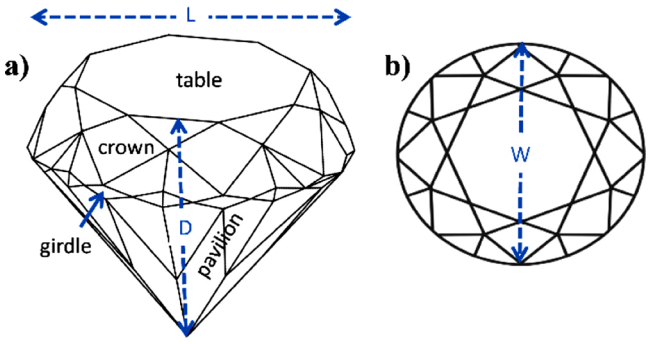

Fig. 1. (a) Line diagram of a typical jeweler's diamond showing its various polished facets, (b) top view; L, D and W vectors define length, depth and width of the diamond.

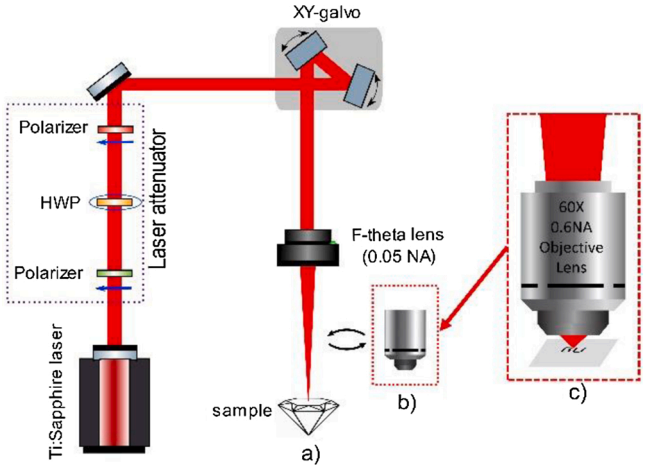

Fig. 2. Experimental schematic of the fs-laser system and optics setup for diamond marking with (a) 0.05 NA f-theta lens, (b) 0.60 NA add-on objective, and (c) magnified view of the laser marking trough the objective lens; HWP is halfwave plate.

the optical path. A focused beam traversed continuously on the sample through the motorized XY-galvo mirrors while the "z" direction was controlled by the stage motion controller.

Laser micro-marking of the diamond was implemented by inserting a 0.60 NA (60X) retractable objective lens into the unfocused beam from the f-theta lens (Fig. 2(c)), allowing the scanning beam from the galvo to fill the objective back aperture and to move within the aperture. The optical design, hereafter referred to as "two-lens focusing system", advanced the focusing capability of the laser system by reducing the original focused spot size to 3 μm (experimentally determined) on the marked specimen enabling writing on the thin facets such as crown, upper girdle and pavilion. The label and the data matrix code required for laser marking were created in the WaveRunner scan control software (Nutfield Technology). A data matrix code (standard ECC 200) with size

Table 1
Reported experimental results on ultrafast fs-laser (700-800 nm, 100-120fs) processing of diamonds.

Pulse energy (μJ)	Freq. (Hz)	Laser intensity (J/cm^2)	f-spot size (μm)	Marking size (μm)	Obj. NA	Diamond type	Ref.
9−100	10	–	10−30	120−240	0.17, 0.4	SCD (n)[a]	[11]
4	1000	2.34	14	432 × 432	0.17	SCD (n)	[12]
400	–	0.3−0.4	3	–	–	SCD (s)[b], SCD (n)	[13]
0.1−1.3	1000	–	2−5	6−13	1.4	SCD (s)	[14]
8−12	5000	2.23−3.82, 169	20, 3	100 × 150, 20 × 25	0.05, 0.6	SCD (n)	this paper

[a] Single crystal diamond (natural).
[b] Single crystal diamond (synthetic).

of 350 × 350 μm^2 was inscribed by scanning the laser beam with, and without the two-lens focusing system. The final marking was successfully decoded as text "DCW" after being scanned by QR Scanner (AO Kaspersky Lab, version 1.4.4.173) i.e. an open source app available on google play store.

The experiments were performed within a range of laser parameters, i.e. pulse energy, galvo scanning speed and number of pass given in Table 2. The laser fluence of ~2.5 J/cm^2 was opted for marking, which also corresponds to the single pulse threshold for diamond ablation [15]. The choice of parameters adopted for laser scanning through two-lens focusing is also given in Table 2. The alphanumeric features were written by continuous scanning of the focused laser beam at variable speed, whereas the data matrix code was inscribed by hatching, i.e. continuous pulsing of the laser beam with overlap. Meanwhile, the laser scanning speed was enhanced to overcome accumulation effect and prevent potential damage to the diamond due to increased laser intensity (decreased focus spot size) through the two-lens focusing system. The scan speed through two-lens focusing, termed as the "effective scanning speed", was calculated as follows;

$$Effective\ \ scanning\ \ speed = distance\ \ between\ \ two\ \ spots\ (\mu m) \times pulse\ \ repetition\ \ rate\ (Hz)$$

For laser pulsing frequency of 5000 pulses/sec, and distance of 2.8 μm measured between two immediate spots on marked region, the effective scanning speed obtained on the diamond is 14 mm/sec, against the original galvo speed of 100 mm/sec, i.e. reducing 7-folds approximately after passing through the 0.6 NA objective.

2.2. Characterization

White-light optical microscopy in bright field/dark field (BF/DF) mode with 10X and 50X magnification objectives was used for imaging the marked diamond surface. The depth profile of laser treated diamond was carried out on a 3D optical microscope (Olympus DSX1000). A detailed morphological examination was performed by Hitachi TM4000 + SEM equipped with both secondary electron (SE) and back-scattered electron (BSE) detectors. The SEM was operated in a low-vacuum mode that enabled direct viewing of the sample without conductive coating. The laser-marked regions were microscopically observed by focusing from top of the sample surface. Raman spectra were obtained using a Bruker Senterra 2 instrument equipped with a 532 nm laser. The power of the laser was 25 mW and a 50 μm aperture with 20X objective to give a 5 μm spot size. An integration time of 5 s was applied with 5 co-additions.

3. Results and discussion

Fig. 3 shows BF optical micrographs and SEM images (BSE mode) of the laser-marked diamond sample. The result from the sample that was laser scanned by a single pass is shown in Fig. 3(a) indicating "BU" inscription on the diamond top facet i.e. the table. The size of the inscribed text is 255 × 155 μm^2 with uniform geometry and line thickness. This agrees to the original size (250 × 150 μm^2) of the plain text outline created in the galvo-scanner software. Thickness of the individual line drawn on the diamond is ~20 μm (±5 %) approximately corresponding to the focussed laser spot size. The unfinished part from the top portion of "B" occurred due to the default delay time between laser start and galvo-scanner movement that was fine tuned in later experiments.

Table 2
Experimental parameters used for laser marking of diamond.

Pulse energy μJ	Focus spot size μm	Laser intensity J/cm^2	Laser scan speed mm/s	No. of pass	No. of pulses/spot	Focusing lens NA
8	20	2.55	2–5	1–2	50	0.05
12	20	3.82	2–5	1	50	0.05
12	3[a]	169	14[b]	1	1	0.05, 0.60

[a] final size (experimental) after two-lens focusing.
[b] effective speed on sample.

The quality of the laser marking and size of the tracks after a single pass is compared with the corresponding SEM micrographs as shown in Fig. 3(b, c) and (e, f). The bright spots in SEM images (encircled in Fig. 3 (c)) are attributed to the putty remains on the sample after cleaning. Fine periodic structuring has been observed with a periodicity below the laser wavelength in the higher magnification images in Fig. 3(c) and (f). This unique nanostructure, termed as the "LIPSS", is a universal phenomenon attributed to the interaction of the polarized ultrashort laser pulse with materials, including diamond [16,17]. The orientation of ripple pattern was perpendicular to the laser beam polarization direction and the period of the structures (distance between consecutive ripples) was much smaller than the laser wavelength i.e. 800 nm. These features are consistent with high spatial frequency LIPSS (HSFL) model for ultrafast laser processing of dielectric transparent materials [18]. The HSFL were observed at laser intensity near to the ablation threshold of diamond (i.e. ~2.5 J/cm^2) and with rest of the laser parameters as given in Table 2.

The ablation in a non-absorbing dielectric, such as diamond, is a complex phenomenon which has been explained through various models including multiple rate equations (MRE) [19,20]. The absorption of focused fs-pulses initiates through nonlinear field ionization (multi-photon absorption and tunneling ionization) and avalanche ionization, resulting in the creation of an electron-ion plasma [21]. Controlling the laser parameters within a narrow range, led to localized morphological changes required to inscribe high-contrast legible features on the natural diamond surface. On the other hand, marking produced by repeated (2×) laser scanning of the text is shown in Fig. 3(d)–(f). Dark colouration and microcracks were clearly visible near the edge of the laser track in the optical image (Fig. 3(d)) and the SEM micrographs (Fig. 3(f)) respectively. In addition, there was slight increase in the line-width that is ascribed to the incubation effect due to accumulated irradiation consistent with the findings of Ionin et al. [11]. Similar results, with microcracks (not shown), were obtained by decreasing the laser scan speed or increasing number of pulses/spot.

The precise origin of microcracking in diamond is under investigation, comparison of results with earlier studies indicate this phenomenon may result from diamond to graphite phase transformation [22] with an associated volume expansion and lattice strain [13] induced by the absorption of fs-pulses and accumulation effect. The clear increase in microcracking in the sample marked with two passes of the laser indicates the role that LIPSS has, possibly by increasing absorption of laser energy in the diamond due to an increase in surface area [23], a change in the material properties (graphitization), pre-existing mechanical deformation (thermal expansion causing plastic deformation), or a syngergystic effect. This is further examined in the Raman spectroscopic study in later section to elucidate the effect of fs-laser scanning on structural properties and phase relationship of the natural diamond.

In the two-pass example microcracks occurred in the mid part of the "B" (arrow marks in Fig. 3(f)) that propagated in the longitudinal and transverse direction to the laser scanning. It may be associated with the cumulative (4×) laser exposure traversed in the middle of the "B" that led to a pronounced incubation effect [13] in this location of the marking also evidenced by a thin dark patch visible in Fig. 3(d). This behaviour was absent for the marking traversed by a single laser pass as per the micrographs shown in Fig. 3(a)–(c).

Fig. 4 shows optical 3D profile of the laser marking traversed by a single laser pass at scanning speed of 2 mm/s and laser fluence of 3.8 J/cm^2. The laser ablation profile yielded uniform edge quality of the track with a bell-shaped crater, which is attributed to the Gaussian beam characteristic of the fs-laser system. Overall, a track with an average width of 20.6 μm and depth of 0.28 μm was obtained, which corresponds

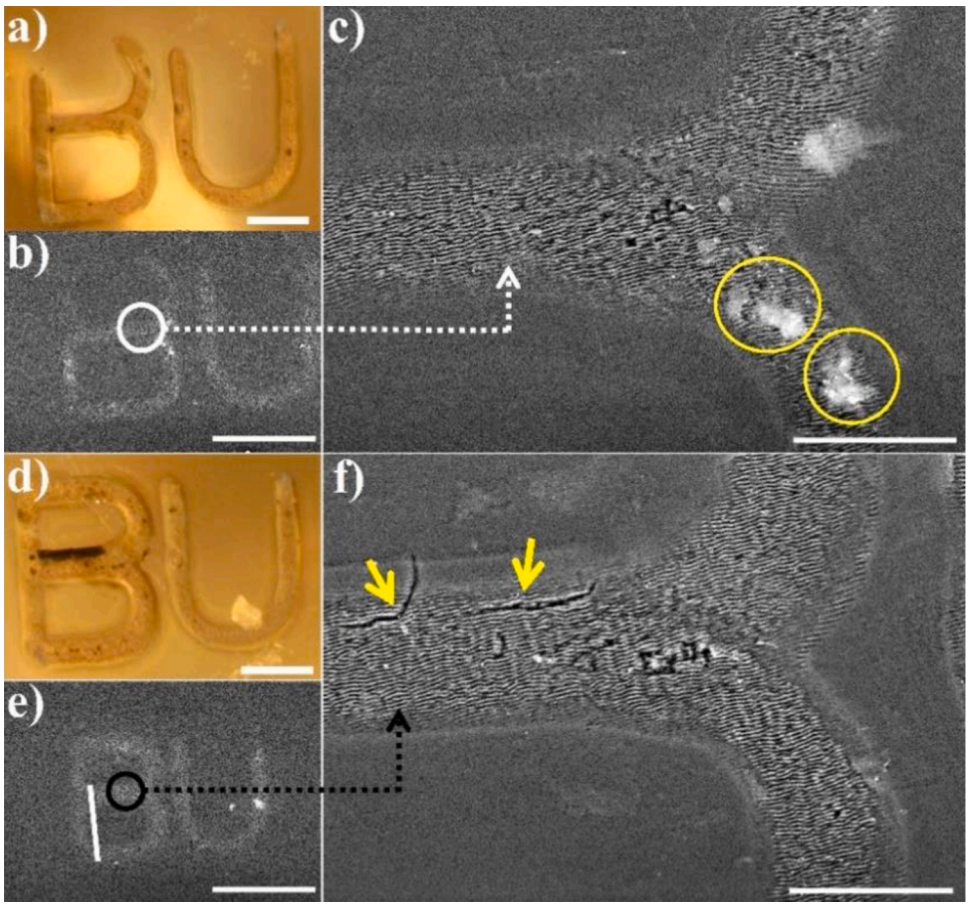

Fig. 3. (a) Optical microscope image of marking produced by single laser pass (scan), (b) corresponding SEM image of laser marking, (c) magnified view of marked area, (d) optical image of marking produced by two laser scans, (e) corresponding SEM image of the laser marking, and (f) High magnification view of the marked area; the scalebar in (a), (d) equals 50 μm, and (b), (e) equals 100 μm, and (c), (f) equals 20 μm; laser pulse intensity through 0.05 NA objective was 2.5 J/cm^2.

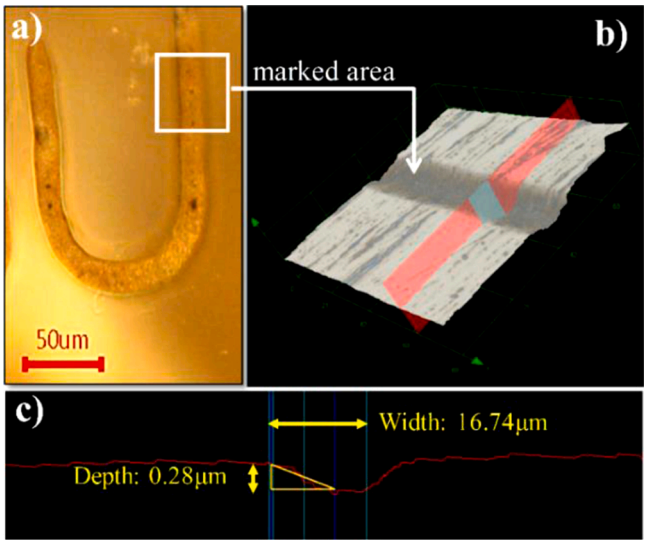

Fig. 4. (a) BF optical micrograph of the diamond marking produced by single laser scan, (b) corresponding 3D optical micrograph, and (c) the depth profile acorss the laser marking.

with the spot size of the laser beam through the original 0.05 NA focusing lens.

Moreover, the fs-laser scanning process was extended to inscribe complex geometry such as data matrix code (350 × 350 μm^2) through the 0.05 NA focusing lens on the marquise diamond. The capability of writing such patterns was evaluated at variable writing speeds through optical microscopy and results are shown in Fig. 5. The surface of the mark generated at scanning speed of 1 mm/s appeared rough and distorted with individual features significantly overlapped (Fig. 5(a)). This is attributed to slow speed of the laser scanning leading to an increased interaction time with the diamond and associated with this is the incubation effect. Meanwhile, microcracking on the edges of the geometry was observed, as encircled in Fig. 5(a). On the other hand, the laser markings inscribed at higher scan speeds yielded different results. Comparing the appearance of data matrix codes, a scan speed of 2−3 mm/s produced the most promising quality of marking without microcracking and substantial darkening of the features in the diamond. In addition, the contrast between the marked and unmarked area was optimum to be recognized by the QR scanner (Fig. 5(e)). A scanning speed of 5 mm/s resulted in reduced sharpness of the developed features, which is ascribed to the inefficient laser absorption, however, it remained readable through the QR scanner.

The result obtained by Raman spectroscopy from laser marked codes at variable writing speeds is shown in Fig. 6. Intense Raman activity observed at 1332 cm^{-1} is attributed to the F_{2g} vibration mode in the bulk untreated sample and linked to the presence of sp^3 bonding in the natural diamond. Raman spectra of laser marked sites (craters) at various scan speeds exhibited the F_{2g} mode as the dominant vibration activity. In order to verify graphitization, typically the D and/or G bands (sp^2 bonding) related to carbon structures (e.g. microcrystalline graphite, amorphous carbon, carbon nanotubes) must be present in Raman spectrum at 1350 cm^{-1} and 1560 cm^{-1} respectively [12]. In this case, a weak hump shaped peak was observed near 1570 cm^{-1} in each laser

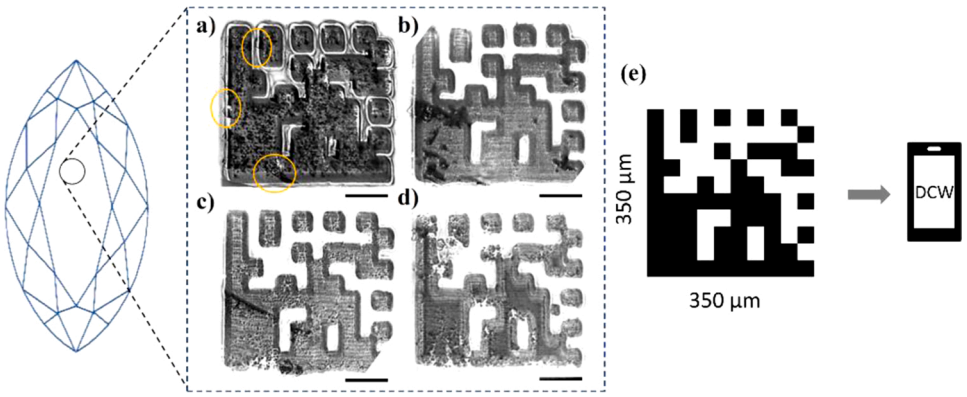

Fig. 5. Comparison of optical micrographsof the laser inscribed code produced at (a) 1 mm/s, (b) 2 mm/s, (c) 3 mm/s, (d) 5 mm/s scanning speed through unaided 0.05 NA lens, and (e) the original data matrix code created in the softwaredecoded as text "DCW" by mobile app; encircled areas in (a) indicate micro-cracks; the scalebar is 100 µm.

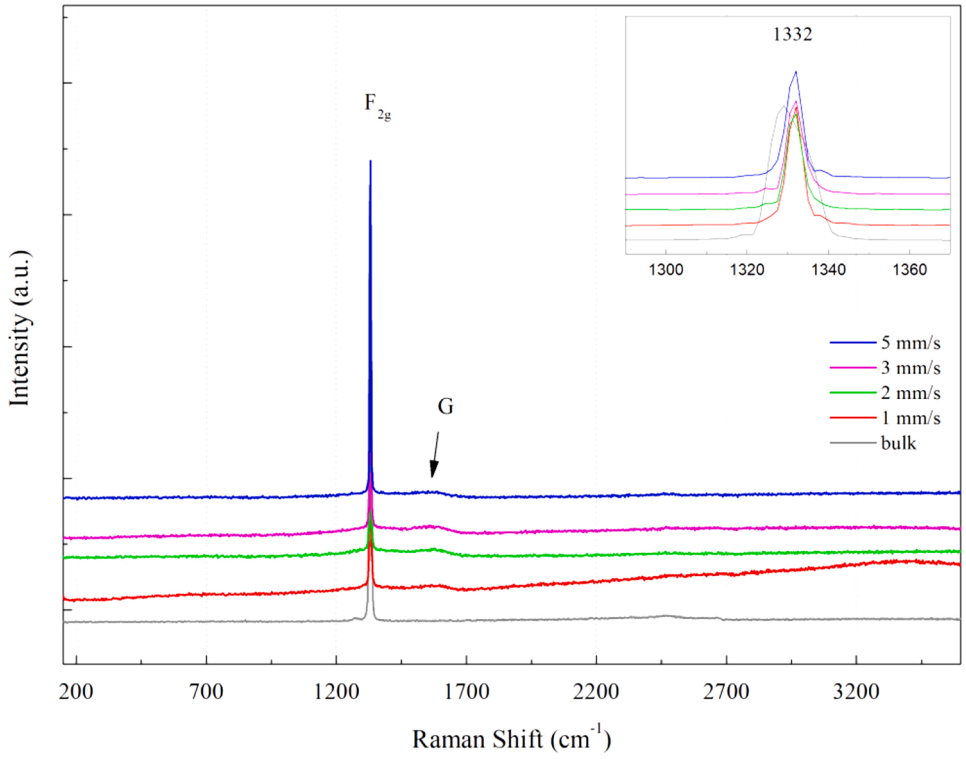

Fig. 6. Raman spectra captured from laser markings produced at variable scanning speeds (through 0.05 NA f-theta lens); inset shows the diamond main peak position in each sample.

scanned area, manifesting local graphitization.

In addition, the main F_{2g} peak in the Raman spectra of laser markings was slightly shifted towards right compared to the peak from untreated bulk diamond as indicated by the inset in Fig. 6. This shift indicates the appearance of compressive stress in the laser modified region in the natural diamond, due to local expansion of the material by the diamond–graphite transition. Comparing the quality of laser markings from Fig. 5 to their corresponding Raman spectra analysis, it is inferred that scan speed between 2−3 mm/s produced the most promising marking without defects i.e. microcracking in the natural diamond. Reducing the scanning speed led to microcracking at the edges of the data matrix code and darkening due to graphitization of the sites by the laser incubation effect. However, increasing scanning speed to 5 mm/s resulted in poor geometry and sharpness of the code due to insufficient laser absorption and nonuniform ablation.

Fig. 7 represents optical micrograph of the laser inscribed serial number in variable size and data matrix code on the emerald diamond produced by fs-laser scanning (1×) through the two-lens focussing system. The polished diamond facet (pavilion) used for the laser marking is indicated in Fig. 7(a), whereas optical micrograph of the full marking is shown in Fig. 7(b). Surface features of the inscriptions (i.e. text and the code) were observed with high-contrast and uniform line thickness without microcracking. The minimum size of the serial number marked as "CPE 003-BU" was approximately 25 µm in height without any overlapping between individual laser spots. Likewise, the size of the data matrix code inscribed on the diamond was $100 \times 100\ \mu m^2$ from the optical micrograph in Fig. 7(b). The line-width of the text marking measured from Fig. 7(c) was ~3 µm, which corresponds to the focused spot-size of laser through two-lens system. This corroborates seven-fold reduction in the focussed beam spot size compared to the original f-theta

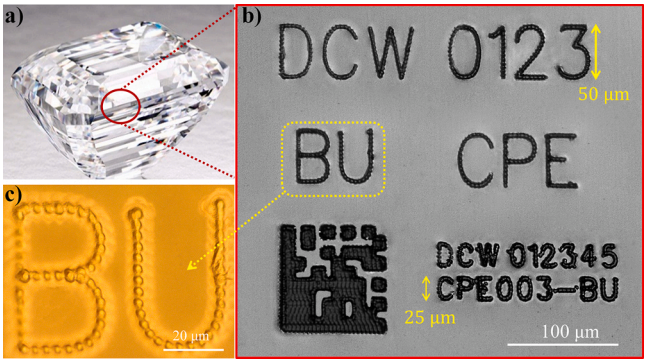

Fig. 7. (a) Optical image of the diamond sample with laser marking, (b) high-contrast optical micrograph of laser inscribed features (code and text) on the diamond produced through two-lens focusing system, and (c) high-magnification optical micrograph of the laser inscribed text labelled in (b).

lens (i.e. 20 µm).

These results demonstrate the role of the two-lens focusing to control the beam spot size and laser scanning to generate interesting security features on natural diamond. This also supports realization of inscribing QR-code like symbols, company logos and alphanumeric serials on natural diamonds with girdle of less than 100 µm across. The remarkable focusing provided by add-on objective was responsible for smaller spot size (compared to the f-theta lens) as well as high-contrast and defect-free laser marking on the diamond. It is noteworthy that the data matrix code in Fig. 7(b) is characterized by a unique substructure formation within the shape boundaries resulting from the continuous laser scanning (hatching) of the geometry and thus absent for the alphanumeric marking. These repeated patterns were larger and appeared dissimilar from the LIPSS observed in our earlier results (Fig. (4)), which may be formed by high scanning speed with tight focusing of the beam through the two-lens system. Its effect on contrast and overall appearance of the barcode is negligible, however, further research will be crucial to elucidate its microstructural identification and the underlying mechanism. On the other hand,the laser marking size can be further reduced to ~230 nm by using the newly developed superlens by the current team [24–26], which is the goal of our next step work.

4. Conclusions

Ultrafast laser inscription of identifiable security-level marking on the surface of natural diamond has been successfully demonstrated in this work. The delivery of fs-laser beam and scanning through a facile two-lens focusing system enabled defect-free marking of legible serial number and data matrix code 25−100 µm in size and only 0.28 µm deep into the surface of the natural diamond. This design allowed high-contrast permanent marking without distortion of features at optimum pulse energy of 12 µJ and scanning speed of 14 mm/s. A remarkable improvement in the resolution of the produced features was demonstrated by the 7× reduction in the line-width of the laser marking. Meanwhile, micro-sized defects such as darkening, microcracking or nonuniform features were generated in the diamond at higher or slower scan speeds and/or repetitive laser scanning of the geometry. The results from this investigation bring new opportunity for the diamond and gemstone businesses for a cost-effective, unaided and machine-readable security markings with single-digit marking resolution.

Funding

Center for Photonics Expertise (CPE) funded by European Regional Development Fund (ERDF) through Welsh Government (81400). SEM work is supported through the Sêr Cymru II programme funded through the Welsh European Funding Office (WEFO) under the ERDF.

CRediT authorship contribution statement

Yasir F. Joya: Methodology, Investigation, Writing - original draft. **Bing Yan:** Methodology, Investigation. **Kelvin James:** Conceptualization. **Liyang Yue:** Methodology. **Simon C. Middleburgh:** Methodology. **Zengbo Wang:** Conceptualization.

Declaration of Competing Interest

The authors declare that they have no known competing financial interests or personal relationships that could have appeared to influence the work reported in this paper.

Acknowledgments

The authors would like to acknowledge the faculty and staff from School of Computer Science and Electronic Engineering at Bangor University who contributed to this project including Mr. Iwan Jones for mechanical workshop and Mr. Ben Assinder for analytical lab work.

References

[1] L.E. Cartier, S.H. Ali, M.S. Krzemnicki, Blockchain, chain of custody and trace elements: an overview of tracking and traceability opportunities in the gem industry, J. Gemmol. 36 (2018) 212–227.
[2] M.S.K, H.A.O. Wang, System for Marking and Analysing Gemstones, EP3305461 A1, 2016.
[3] Ralph Delmdahl, Smarter Lens Marking with the 193 Nm Excimer Laser: a Single Solution to Meet the Demands of a Changing Market, C. Int., 2018, p. 1. htt p://www.cmmmagazine.com/cmm-articles/smarter-lens-marking-with-the-193-nm-excimer-laser-a-single-/.
[4] S. Gloor, W. Lüthy, H.P. Weber, Submicron laser writing on diamond, Diam. Relat. Mater. 8 (1999) 1853–1856.
[5] M.S. Komlenok, V.V. Kononenko, V.G. Ralchenko, S.M. Pimenov, V.I. Konov, Laser induced nanoablation of diamond materials, Phys. Procedia 12 (2011) 37–45.
[6] R.R. Gattass, E. Mazur, Femtosecond laser micromachining in transparent materials, Nat. Photonics 2 (2008) 219–225.
[7] M. Malinauskas, A. Žukauskas, S. Hasegawa, Y. Hayasaki, V. Mizeikis, R. Buividas, S. Juodkazis, Ultrafast laser processing of materials: from science to industry, Light Sci. Appl. 5 (2016) e16133.
[8] V.I. Konov, Laser in micro and nanoprocessing of diamond materials, Laser Photon. Rev. 6 (2012) 739–766.
[9] D.M. Trucchi, A. Bellucci, M. Girolami, M. Mastellone, S. Orlando, Surface texturing of CVD diamond assisted by ultrashort laser pulses, Coatings 7 (2017) 185.
[10] T.V. Kononenko, M.S. Komlenok, V.P. Pashinin, S.M. Pimenov, V.I. Konov, M. Neff, V. Romano, W. Lüthy, Femtosecond laser microstructuring in the bulk of diamond, Diam. Relat. Mater. 18 (2009) 196–199.
[11] A.A. Ionin, S.I. Kudryashov, K.E. Mikhin, L.V. Seleznev, D.V. Sinitsyn, Bulk femtosecond laser marking of natural diamonds, Laser Phys. 20 (2010) 1778–1782.
[12] A.J. Batista, P.G. Vianna, H.B. Ribeiro, C.J.S. de Matos, A.S.L. Gomes, QR code micro-certified gemstones: femtosecond writing and Raman characterization in Diamond, Ruby and Sapphire, Sci. Rep. 9 (2019) 8927.
[13] T.V. Kononenko, M. Meier, M.S. Komlenok, S.M. Pimenov, V. Romano, V. P. Pashinin, V.I. Konov, Microstructuring of diamond bulk by IR femtosecond laser pulses, Appl. Phys. A. 90 (2008) 645–651.
[14] R.D. Simmonds, P.S. Salter, A. Jesacher, M.J. Booth, Three dimensional laser microfabrication in diamond using a dual adaptive optics system, Opt. Express 19 (2011) 24122–24128.
[15] P. Boerner, M. Hajri, N. Ackerl, K. Wegener, Experimental and theoretical investigation of ultrashort pulsed laser ablation of diamond, J. Laser Appl. 31 (2019) 22202.
[16] J. Bonse, S. Höhm, S.V. Kirner, A. Rosenfeld, J. Krüger, Laser-induced periodic surface structures— a scientific evergreen, IEEE J. Sel. Top. Quantum Electron. 23 (2017) 1.
[17] M. Shinoda, R.R. Gattass, E. Mazur, Femtosecond laser-induced formation of nanometer-width grooves on synthetic single-crystal diamond surfaces, J. Appl. Phys. 105 (2009) 53102.
[18] A. Abdelmalek, B. Sotillo, Z. Bedrane, V. Bharadwaj, S. Pietralunga, R. Ramponi, E.-H. Amara, S.M. Eaton, Origin of femtosecond laser induced periodic nanostructure on diamond, AIP Adv. 7 (2017), 105105.
[19] B.H. Christensen, P. Balling, Modeling ultrashort-pulse laser ablation of dielectric materials, Phys. Rev. B 79 (2009), 155424.
[20] S.S. Mao, F. Quéré, S. Guizard, X. Mao, R.E. Russo, G. Petite, P. Martin, Dynamics of femtosecond laser interactions with dielectrics, Appl. Phys. A. 79 (2004) 1695–1709.
[21] K. Itoh, W. Watanabe, S. Nolte, C.B. Schaffer, Ultrafast processes for bulk modification of transparent materials, MRS Bull. 31 (2006) 620–625.

[22] S. Su, J. Li, G.C.B. Lee, K. Sugden, D. Webb, H. Ye, Femtosecond laser-induced microstructures on diamond for microfluidic sensing device applications, Appl. Phys. Lett. 102 (2013), 231913.
[23] P. Calvani, A. Bellucci, M. Girolami, S. Orlando, V. Valentini, A. Lettino, D. M. Trucchi, Optical properties of femtosecond laser-treated diamond, Appl. Phys. A. 117 (2014) 25–29.
[24] B. Yan, L. Yue, J.N. Monks, X. Yang, D. Xiong, C. Jiang, Z. Wang, Superlensing Plano-Convex-Microsphere(PCM) lens for direct laser nano marking and beyond, Opt. Lett. 45 (2020) 1168–1171.
[25] B. Yan, Y. Song, X. Yang, D. Xiong, Z. Wang, Unibody microscope objective tipped with a microsphere: design, fabrication and application in subwavelength imaging, Appl. Opt. 59 (2020) 2641–2648.
[26] Z. Wang, B.S. Luk'yanchuk, Super-Resolution Imaging and Microscopy by Dielectric Particle-Lenses, in Book Label-Free Super-Resolution Microscopy, Springer, 2019. ISBN 978-3-030-21722-8.